

UCRL- 90279
PREPRINT

CIRCULATION COPY
SUBJECT TO RECALL
IN TWO WEEKS

Observation of Amplification of the OVIII H α Line In A
Recombining Laser-Produced Plasma

D. L. Matthews, E. M. Campbell, K. Estabrook, W. Hatcher,
R. L. Kauffman, R. W. Lee, and C. L. Wang

Applied Physics Letters

January 1, 1984

Lawrence
Livermore
National
Laboratory

This is a preprint of a paper intended for publication in a journal or proceedings. Since changes may be made before publication, this preprint is made available with the understanding that it will not be cited or reproduced without the permission of the author.

DISCLAIMER

This document was prepared as an account of work sponsored by an agency of the United States Government. Neither the United States Government nor the University of California nor any of their employees, makes any warranty, express or implied, or assumes any legal liability or responsibility for the accuracy, completeness, or usefulness of any information, apparatus, product, or process disclosed, or represents that its use would not infringe privately owned rights. Reference herein to any specific commercial products, process, or service by trade name, trademark, manufacturer, or otherwise, does not necessarily constitute or imply its endorsement, recommendation, or favoring by the United States Government or the University of California. The views and opinions of authors expressed herein do not necessarily state or reflect those of the United States Government thereof, and shall not be used for advertising or product endorsement purposes.

162 142
C. J.

Observation of Amplification of the OVIII H α Line In A
Recombining Laser-Produced Plasma*

D. L. Matthews, E. M. Campbell, K. Estabrook, W. Hatcher
R. L. Kauffman, R. W. Lee, and C. L. Wang

Lawrence Livermore National Laboratory
Livermore, California 94550

Abstract

We have observed enhanced emission of the O VIII H α line at 121 eV from a recombining plasma produced by laser heating of a thin Formvar foil with two opposed cylindrically-focused (0.3 x 1.4 cm) 5 TW laser beams. The time-dependent intensity of the H α line increases by nearly an order of magnitude as the plasma length is increased from 0.27 to 1.27 cm. This increase in intensity is greater than that expected from a medium exhibiting no gain. A comparison of the measured time history of the emission with that of non-LTE time-dependent calculations suggests that a small signal gain $\sim 0.5 \text{ cm}^{-1}$ is obtained.

*Work performed under the auspices of the U. S. Department of Energy by the Lawrence Livermore National Laboratory under contract number W-7405-ENG-48.

It has long been recognized that population inversions between electronic states in an ion can be created by three-body recombination-cascade in a relaxing plasma.⁽¹⁾ The technique can be extended to the XUV or soft x-ray region using laser-heated plasmas by irradiating targets at high-intensity. The rapid cooling associated with adiabatic expansion of the heated plasma can lead to conditions favorable for a recombination laser.^(2,3)

Several authors have reported population inversion⁽⁴⁾ or gain^(5,6) in the XUV region using laser-produced plasmas in various geometries. These experiments are difficult because of the relatively low signals from the plasma, due to the limited size of the incident laser. In addition, all of the measurements are time-integrated which can confuse interpretation, since most theories⁽⁷⁾ do not predict gain to occur over the entire emission lifetime of the plasma.

Despite these complexities, the recombination scheme remains a theoretically interesting problem with gains as high as 10 cm^{-1} predicted for certain schemes which are optimized and pumped by a high energy laser.

In the present work we investigate the recombination lasing scheme and measure a small gain on the Balmer alpha line of O VIII for a laser-heated Formvar foil. Using the Novette laser operated at green ($0.53 \mu\text{m}$) wavelength at 5 TW/beam power levels we have been able to obtain sufficient signal in a single shot to facilitate both

time-resolved and time-integrated measurements along opposite lines-of-sight of the axial xray emission. The intensity of the H α line was monitored as a function of time for plasma lengths from 0.27 to 1.27 cm. The plasma was formed by two opposed cylindrically-focused (0.3 x 1.4 cm) laser beams. The simple ratio of intensity from long to short plasmas was greater than can be expected without considering amplified spontaneous emission. Comparison of the time-dependent intensity measurement with that of some time-dependent calculations has indicated that the gain peaks roughly 1 nsec after the heating laser pulse at values of order 0.5 cm^{-1} .

A schematic representation of the experiment is shown in Fig. 1. We have irradiated a thin 2000 Å-thick Formvar foil (atomic percentage of oxygen is $\sim 13\%$) with two opposed cylindrically focused (1.4 cm x 0.3 cm) laser beams from the frequency-doubled ($\lambda_L = 0.53 \mu\text{m}$) Nd-Glass laser at the Novette facility. Total power in each beam is 5 TW, at a pulse duration of 100 ps FWHM, which produces an average irradiance at the surface of the foil of $1.4 \times 10^{13} \text{ W/cm}^2$. Given the dimensions, the plasma is essentially planar during the course of the experiment.* While not maximizing the cooling rate, the experiment geometry simplifies 1D simulations, and the shallow density gradients minimize xray refraction over the long path lengths in the plasma. Calculations predict that these heating conditions rapidly ionize the Formvar foil. Rapid

*Calculations indicate that the foil expands 100-200 μm along the laser direction in the time scales of interest. Thus the hydrodynamic cooling of the plasma will be similar for the plasma lengths examined in these experiments.

adiabatic decompression, hence cooling, can then occur, thus the foils will physically explode due to its rapid bulk heating (foil is thin compared to the laser ablation depth). No special target construction is attempted to induce additional cooling mechanisms, such as radiation or electron conduction.

The O VIII H α line (3-2) was measured by two spectrographs viewing opposite ends of the irradiated Formvar foil. One instrument provided a time-resolved spectral measurement by combining a streak camera and a free-standing transmission grating. This spectrograph time-resolves portions of the x-ray spectrum in the range from 50 eV to 150 eV with a resolving power ($E/\Delta E$) of 200 at 121 eV and with a temporal resolution of 20 psec FWHM. Details of the instrument are presented elsewhere.⁽⁸⁾ A sample of the film data obtained with this instrument is shown in Fig. 1. Here we display the x-ray spectrum vs. time in the vicinity (centered on the film) of the O VIII H α line. A time-integrated, grazing incidence spectrograph viewed the line-of-sight opposite to the time-resolving transmission-grating spectrograph. The time-integrated instrument had relatively low resolving ($\lambda/\Delta\lambda \sim 50$) and was primarily intended to provide broad energy coverage and insensitivity to target pointing inaccuracies. In the data discussed here this instrument corroborates the time-resolved measurements and spectral line identifications.

We irradiated three different lengths of Formvar foils, one having a 1.27 cm active length and two other targets having 0.32 and 0.27 cm lengths, respectively, holding constant all other irradiation conditions. The experimental method determines if exponential amplification in the line intensity is occurring by comparing the

relative emission in the axial (longitudinal) direction for a long and a short target. Excluding opacity effects (which we discuss below) the total time-integrated intensity should only increase as the length of the target, i.e., if no amplification is occurring. Two-dimensional effects on signal strengths are minimized by holding laser irradiation conditions constant (thus plasma expansion velocities and cooling rates should be nearly the same) and by placing 2 mm-diameter collimators at either end of the target to restrict the diagnostics viewing region to the central portion of the plasma. Also, the beams overfilled the ends of the foils, eliminating absorption by colder plasma at the edges of the beams. Alignment of the potential lasing volume to our diagnostics is accomplished using an auto collimation technique which assures the pointing accuracy of the longitudinal axis of the plasma to ± 0.5 mrad.

Examples of the time-resolved data for the long and short target are shown in Fig. 1. In Fig. 2. we display the intensity vs. time for the H α line as well as the time behavior of the nearby continuum, i.e., xray emission at wavelength near the H α line but not including it or any other discernible transition. The relative timing between curves from different laser shots (i.e., long and short foil cases) is determined by normalizing to the peak of the bremsstrahlung emission, which occurs at a time corresponding to the peak of the incident laser heating pulse.

Concentrating on the emission characteristics of the H α line as a function of time, we observe two interesting results. First, the early time behavior of the short and long foil cases are very similar. This is

consistent with the line being optically thick during the heating laser pulse. During the time the plasma is hot and dense, they should thus exhibit approximately the same brightness. Second, at later times when the plasma decompresses and the level inversions fully develop, the effect of the amplification becomes more evident. At times on the order of 1.0 ns, it is evident from both Fig. 1 and Fig. 2 that the long foil case is still emitting near peak brightness, whereas the brightness of the short foil emission is indistinguishable from film noise and x-ray background. A simple determination of the gain coefficient $\alpha(\text{cm}^{-1})$ can be directly obtained from the ratio of the measured brightness B of the H_α emission for the long-to-short foil cases. Ignoring time-dependent effects of opacity of the H_α line and presuming the measured line brightness can be separated from continuum contributions

$$\frac{1 - e^{-\alpha[\text{Length of Longfoil}]}}{1 - e^{-\alpha[\text{Length of Shortfoil}]}} = \frac{B_{\text{Long}}}{B_{\text{Short}}} \quad (1)$$

For example, the ratio appears to peak at $t \sim 800$ psec at the value of approximately 5.6, resulting in $\alpha \approx 0.5 \text{ cm}^{-1}$. The simple estimate is apparently fairly accurate since a comparison to a theoretical prediction (to be described shortly) gives a similar value for the gain.

Comparison of the measured line brightness to that of the corresponding continuum illustrates two other important phenomena.

First, the continuum peaks in brightness earlier in time than does the line emission. This is to be expected due to the different mechanisms responsible for the bremsstrahlung vs. bound-bound emission processes. The bremsstrahlung essentially tracks the laser heating intensity, because the matter temperature and density, both of which couple to give emission, are then highest. The line, or bound-bound emission, peaks somewhat later because of opacity effects and the slower rates of recombination into the $n=3$ level. Comparing the continuum for long and short foil cases illustrates that the continuum is optically thick at early times, which would also negate a linear scaling in brightness with plasma length. These complicated emission dynamics illustrate the necessity of diagnosing such experiments with time-resolving diagnostics.

Comparison of theoretical modeling of the intensity vs. time with the data supports our simple conclusion of the observation of gain. We have modelled the x-ray emission by performing time-dependent simulations of the hydrodynamics and coupling these with the history of the level populations of the important transitions. The critical assumptions are that the hydrodynamics do not depend on the details of the level populations. This allows us to use a simulation code which includes non-LTE physics, but not detailed level populations for the lithium-, helium-, and hydrogen-like oxygen lines. We use the results of the hydrodynamic simulation to drive a set of detailed rate equations which solve for the level populations as a function of time. Next, we assume that the gain will always be small, so that the signal is assumed to be calculable by the usual radiative transfer methods, allowing the optical

depth to be either negative or positive. This decouples the rate equations from the radiation transfer equation, a procedure which should be valid if the gain is very much below saturation. Finally, we assume that optical depth effects, especially critical in the Lyman- α transition, can be modeled by escape factors. This last assumption is not critical because the optical depth, τ_α , in the Lyman- α line is quite small ($\tau_\alpha < 1$) at times of peak gain and increases only near the end of the observation time ($\tau_\alpha \sim 1$).

To perform the hydrodynamic calculations we use LASNEX⁽⁹⁾ (a code which simulates laser-plasma interactions and plasma dynamics) with non-LTE rate equations to produce a hydrodynamic time history.

Calculational uncertainties in the laser plasma coupling, energy transport and hydrodynamics should be small, due to the low intensity on target and small value of $I\lambda^2$ ($I\lambda^2 < 4 \times 10^{12} \text{ W/cm}^2$). The rate equation model that solves for the level populations is based on a complete model of the lithium, helium, and hydrogenic state with the other ionization stages included, using a set of hydrogenic-type levels with the corrected ionization potentials.⁽¹⁰⁾

The results of the calculation are shown in Fig. 3, where we compare the theory to the experiment for the running integral, i.e., the time-dependent total emission observed for the two experimental cases. Note the good agreement. The calculations are normalized to the integral over time of the 0.27 cm experimental results. The spontaneous emission level indicated in Fig. 3 is the calculated output from the 1.27 cm foil when the absorption coefficient is artificially restricted to negative values. The experiment is above this value, confirming that gain

(positive absorption) is required to explain the observations. We have estimated the sensitivity to the theoretical modeling, by varying the electron temperature in the hydrodynamics model by 10 %. As expected for a recombining plasma, the results are indeed sensitive to the details of the temperature history with 10 % difference in T_e leading to greater than 10 % in the emission. Most importantly, we have a system which does not depend on the details of many rate coefficients, but which does show gain, as well as time dependence in the gain. This comparison indicates that time resolution in both the data and calculations is needed and that small gains can be studied. The peak gain-length predicted here is $\alpha L \approx 0.6$.

In summary, we have observed enhanced emission from the O VIII H α line, consistent with amplified spontaneous emission with a gain of 0.5 cm^{-1} . The experimental method was simple, namely we measured the axial line emission from a plasma produced by laser heating of a thin Formvar foil whose length was varied to test for signal amplification. The gain can be directly determined by comparing measured brightness values to those observed from a medium exhibiting little or no gain. Furthermore, the use of a large laser irradiance area ($0.3 \text{ cm} \times 1.4 \text{ cm}$) increased x-ray yields so that multiple shots were not required. The implementation of a time-resolved diagnostic allows for direct study of emission time history and indicates that peak gains are higher than time-averaged values. Meaningful comparison to a hydrodynamics-ionization kinetics code are also facilitated by measuring the emission time history.

Numerous experimental improvements can be made to increase amplification of the O VIII H α line. Modification of the laser optics

to provide a 3 cm-long line focus will further check the exponentiation of signal strength with gain length (provided refraction can be controlled). In addition, calculations suggest that changing to a shorter pump laser wavelength, namely $\lambda_L = 0.35 \mu\text{m}$, may increase the gain by approximately 30%.

References:

1. L. I. Gudzenko and L. A. Shelepin, Sov. Physx. JETP 18,998(1964);
Sov. Phys. - DOKL. 10,147(1965).
2. G. Pert, J. Phys B9,330(1976).
3. A. Vinogradov and I. Sobel'man, Zh. Eksp. Teor. Fiz. 63,2113; Sov.
Phys. JETP 36,115(1973).
4. F. Irons and N. Peacock, J. Phys. B7,1109(1974).
5. R. Dewhurst, D. Jacoby, G. Pert, and S. Ramsden, Phys. Rev. Lett.
37,1265(1976).
6. D. Jacoby, G. Pert, S. Ramsden, L. Shorrock, and G. Tallents
37,193(1981).
7. G. Pert and G. Tallents, J. Phys. B14,1525(1981).
8. To be published, R. Kauffman.
9. G. B. Zimmerman and W. L. Kruer, Comments Plasma Physics 2,85(1977).
10. R. W. Lee, Journal of Quantitative Spectroscopy and Radiative
Transfer 27,87(1981).

Figure Captions

1. Experimental Setup for the recombination xray laser measurements; actual prints of the xray streak camera film data are shown for the long and short foil cases.
2. Densitometer traces of the film data shown in Figure 1 illustrates radically different time histories for the long and short foil cases. The long foil (1.27 cm) case is shown by the open circles and the corresponding continuum, i.e., emission at energies just above and below the H_{α} transition is identified on the figure. The short foil emission (0.27) is shown by the open squares and the continuum near the peak is also identified. Emission levels at or near 1.0 are indistinguishable from noise on the film and from other sources.
3. This is a comparison of the running integral of emission intensity between theory (dashed line) and experiment for the long and short foil cases. Also identified on the plot is the result from the time-integrated grazing incidence spectrograph shown with an open square. Finally, the predicted intensity level to be expected from spontaneous emission only without gain is labeled on the graph.

EXPERIMENTAL SETUP FOR THE RECOMBINATION LASER EXPERIMENT

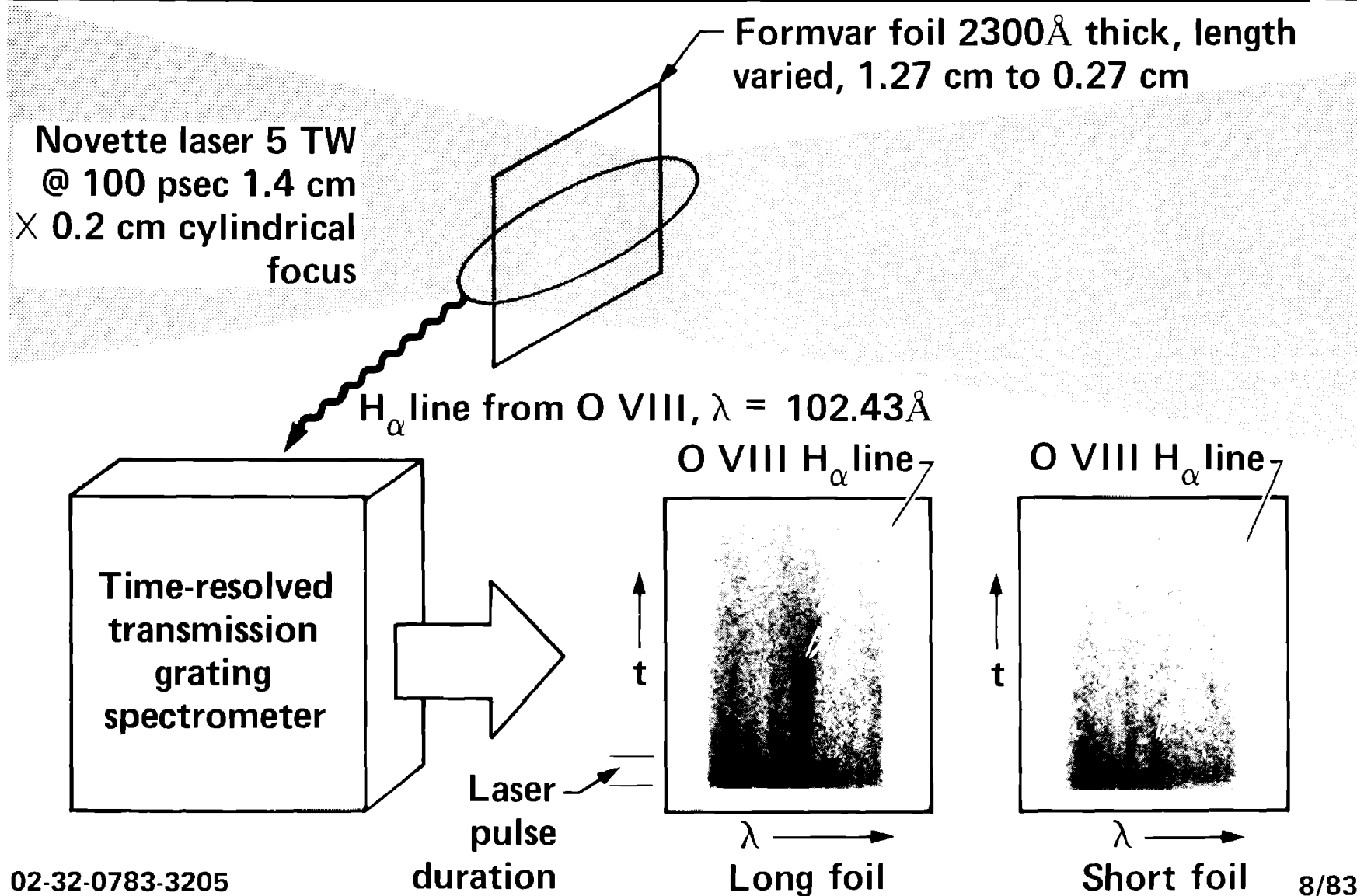


Figure 1

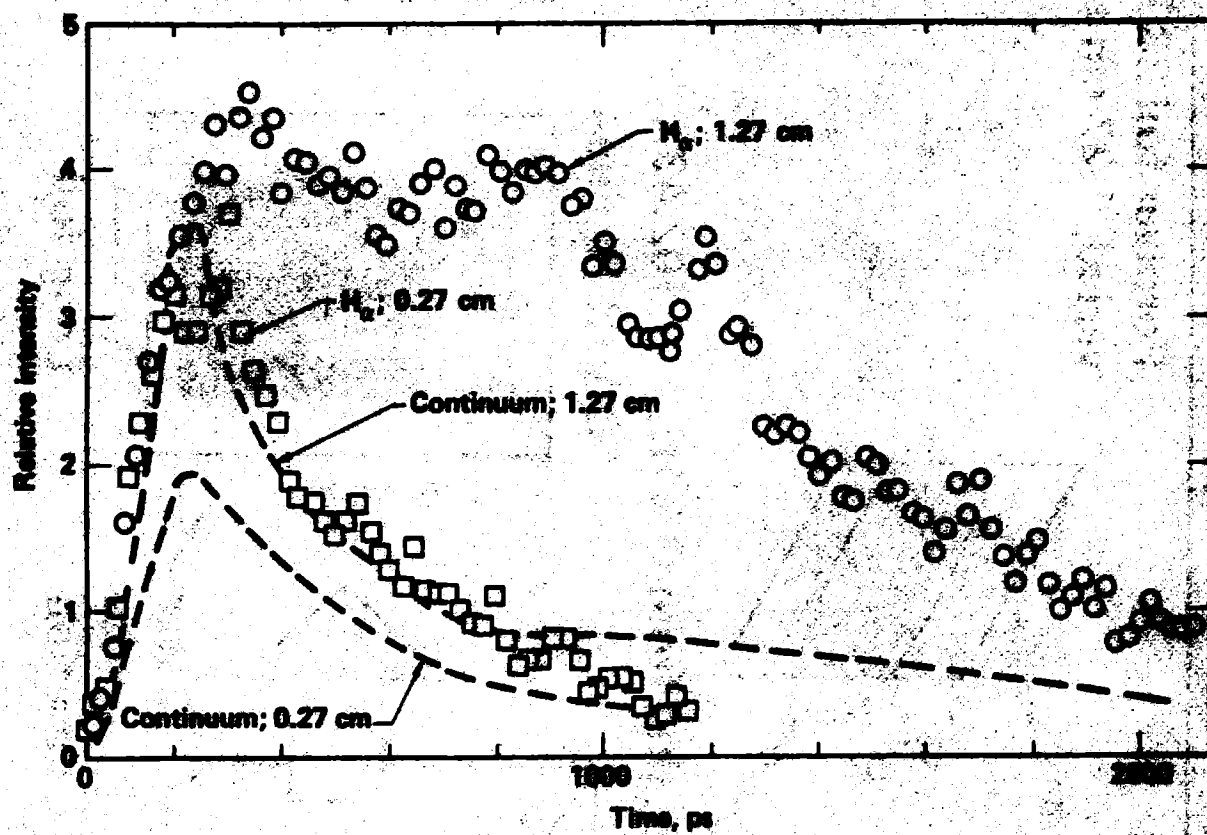


Figure 2

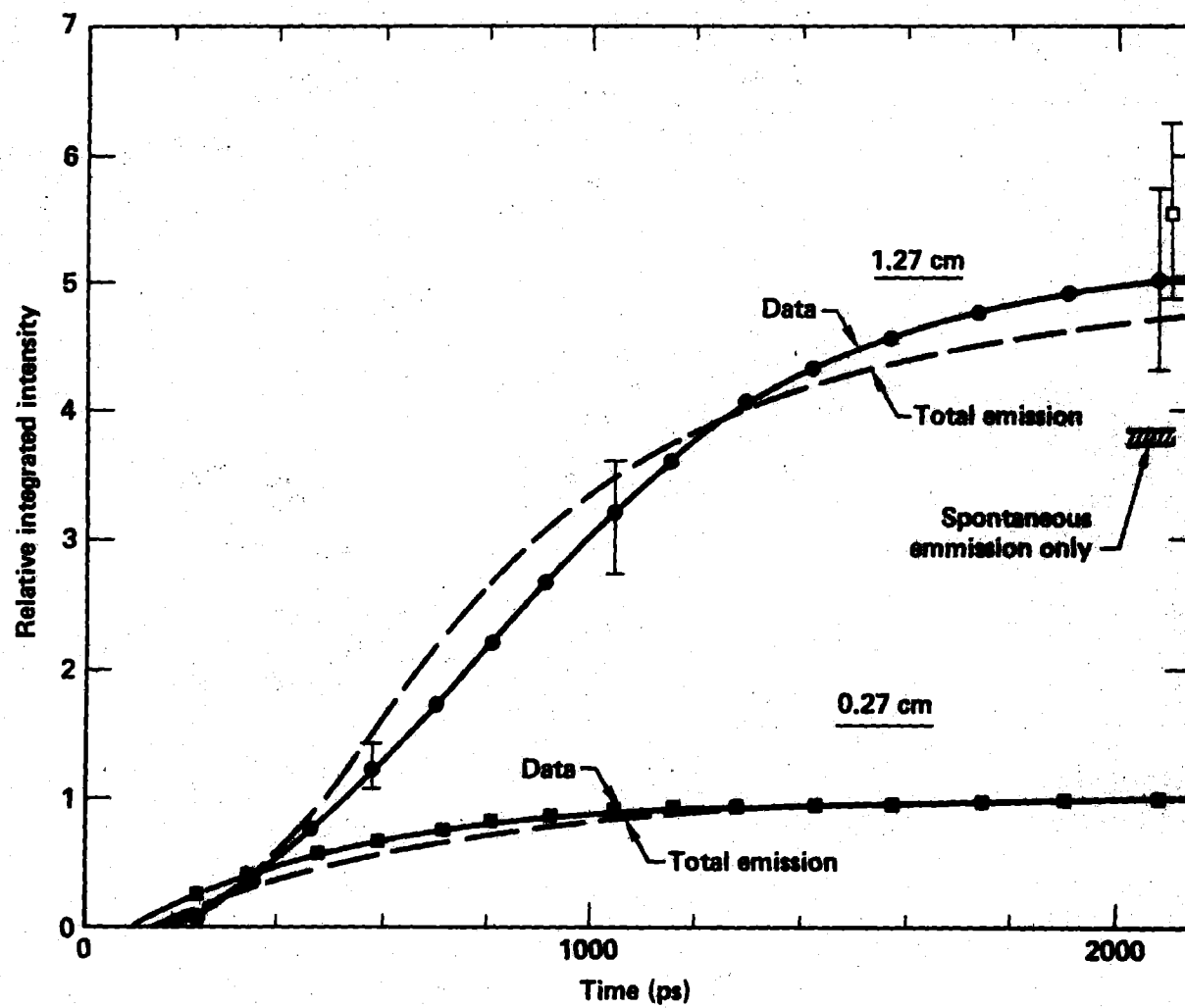
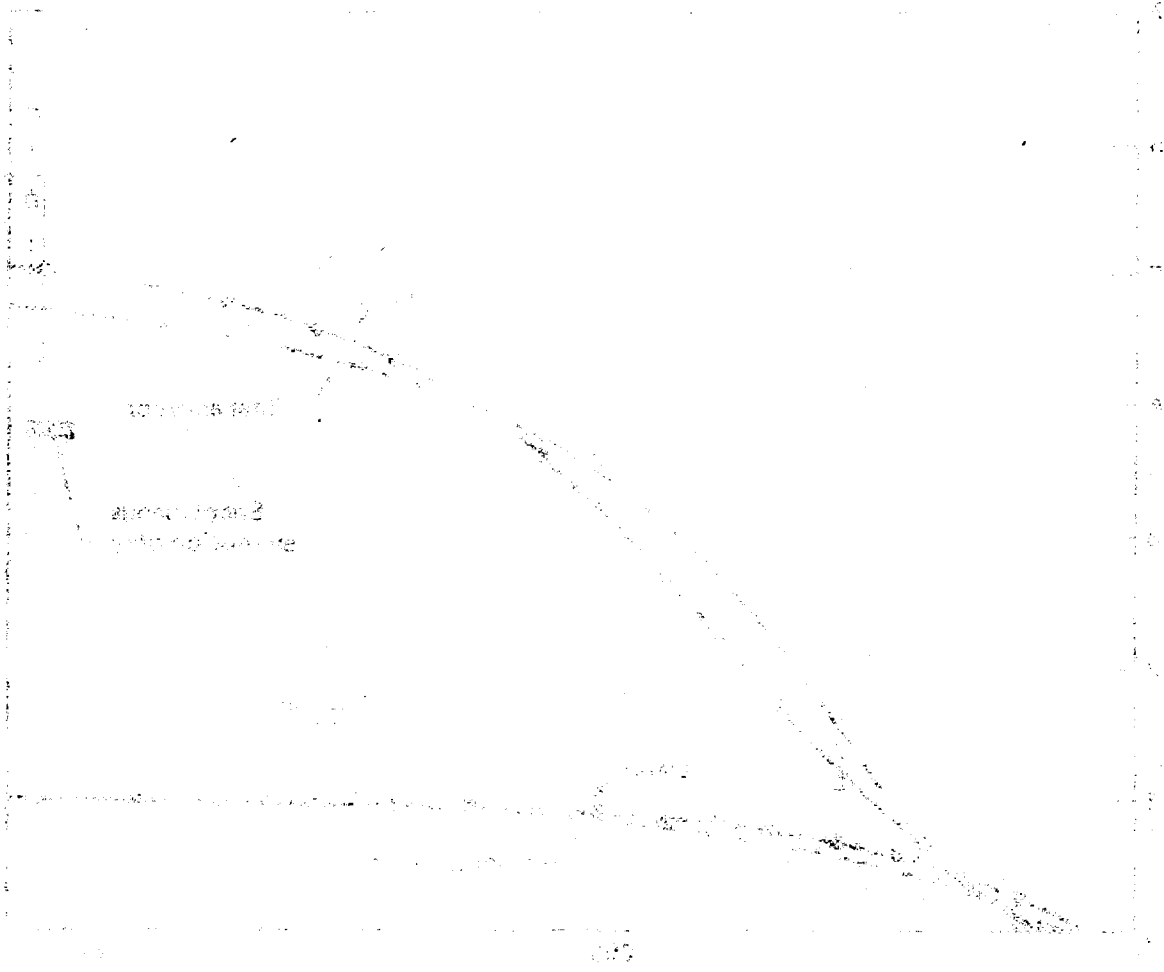


Figure 3



Y-axis label: Value

X-axis label: Time